International Conference on Applied Energy 2019
Aug 12-15, 2019, Västerås, Sweden
Paper ID:1028

A CORRELATION FOR HEAT TRANSFER AND FLOW FRICTION CHARACTERISTICS OF SPIRAL-WOUND HEAT EXCHANGERS

Guo-Yan Zhou[1], Jiaqi Cai[1], Xinghui Gao[1], Shan-Tung Tu[1], Jinguo Zhai[2]

1 Key Laboratory of Pressure Systems and Safety(MOE), School of Mechanical and Power Engineering, East China University of Science and Technology, Shanghai 200237, PR China

2 Shanghai Research Institute of Chemical Industry, Shanghai 200062, PR China

ABSTRACT

Spiral-wound heat exchanger is high-efficiency, intensive, energy-saving heat exchange equipment with compact structure and widely used in petrochemical, nuclear energy and LNG industries. Due to the complicated internal winding of the tubes, heat transfer in the shell side of spiral wound tube heat exchangers has not been sufficiently studied and typical correlations available in the literature are limited in practical applications. This study presents the results of a numerical model developed to analyze the fluid flow and heat transfer inside the spiral-wound heat exchanger of nuclear power systems. The study covered a wide range of operating conditions and geometric parameters, allowing the sensitivity analysis of heat transfer and friction performance to structural parameters and the proposal of a new heat transfer correlation for spiral-wound heat exchangers, which is compared with other correlations adopted in the literature.

Keywords: *Spiral-wound heat exchanger, Heat transfer, Numerical simulation; heat transfer and friction correlation*

NONMENCLATURE

Abbreviations	
APEN	*Applied Energy*
Symbols	
n	*Year*

1. INTRODUCTION

Spiral-wound heat exchanger is high-efficiency, intensive, energy-saving heat exchange equipment with compact structure and widely used in petrochemical, nuclear energy and LNG industries[1-4]. Due to the complicated internal winding of the tubes, the process design calculation method of spiral-wound heat exchanger has not been standardized, which hinder the efficient design and reliable application of the spiral-wound heat exchanger.

The nuclear power plant system typically consists of three loops. Spiral-wound heat exchanger is one of the key components of the reactor coolant pump seal system in the primary loop. Typical correlations available in the literature are limited in practical applications, Based on this, many researches have been carried out to study on the correlations for spiral-wound heat exchanger.

Yang et al.[5] studied the enhanced heat transfer characteristics on the shell side of spiral-wound heat exchanger by experiments. It was found that the working pressure has the greatest influence on the heat transfer characteristics, and the Nu-Re correlation was fitted. Dravid et al.[6] studied the effect of secondary flow on heat transfer in laminar flow through numerical simulation. Based on the simulation results, Nusselt number Nu correlation (1-1) for characterizing heat transfer capacity was proposed as follows:

$$\mathrm{Nu} = (0.65\sqrt{\mathrm{De}} + 0.76)\,\mathrm{Pr}^{0.175} \qquad (1\text{-}1)$$

De ($\mathrm{De} = \mathrm{Re}\sqrt{d/D}$)characterize the centrifugal force and inertial force. Srbislav et al.[7] discussed the influence of the structural parameters such as the axial and radial spacing and winding angle of the wound tube on the heat transfer performance of the shell side through experiments. Based on the experimental results, the correlation of Nusselt number (1-2) was fitted:

$$\mathrm{Nu} = 0.5\mathrm{Re}^{0.55}\,\mathrm{Pr}^{1/3}\left(\eta/\eta_w\right)^{0.14} \qquad (1\text{-}2)$$

Rahul et al.[8] studied the heat transfer performance of the flue gas side of the spiral-wound heat exchanger by experimental and numerical simulation method. The

Selection and peer-review under responsibility of the scientific committee of the 11th Int. Conf. on Applied Energy (ICAE2019).

effects of the structural parameters such as the diameter of the wound tube on the heat transfer process were discussed. According to the results of numerical calculation, the correlation formula (1-3) of heat transfer coefficient of flue gas side was fitted, and the error between the formula and the experimental value was 3-4%.

$$\mathrm{Nu} = 0.0265\,\mathrm{Re}^{0.835}\,\mathrm{Pr}^{0.3}(Gratio)^{-0.097} \qquad (1\text{-}3)$$

In his book "Handbook of Heat Exchanger Design", Oi Hua Ying-lang[9] explained the calculation of heat transfer coefficients in the shell side of the spiral-wound heat exchanger. The calculation of heat transfer coefficient in shell side is based on the calculation method proposed by P. V. Gilli[10]. Nu and f formula is as follows:

$$\mathrm{Nu}=0.664\cdot\mathrm{Re}^{0.5}\cdot\mathrm{Pr}^{0.333} \qquad (1\text{-}4)$$

When Re ≥ 2000, Nu is calculated as follows:

$$\mathrm{Nu}=0.338\cdot F_{\mathrm{t}}\cdot F_{\mathrm{i}}\cdot F_{\mathrm{n}}\cdot\mathrm{Re}^{0.61}\,\mathrm{Pr}^{0.333} \qquad (1\text{-}5)$$

In the formula, F_n, F_t and F_i are the correction coefficients of the tubes.

$$\Delta P=0.334\cdot C_t\cdot C_i\cdot C_n\cdot\frac{n\cdot G^2}{2\rho} \qquad (1\text{-}6)$$

Typical correlations available in the literature do not include structural parameters and have a small scope of application. It is difficult to apply to spiral-wound heat exchanger of nuclear power systems with large operating conditions or specific structural parameters. Therefore, the influence of structural parameters on heat transfer and resistance performance of shell side is analyzed in this paper by CFD method. Based on the numerical results, the new heat transfer correlations of shell side are established, which provide guidance for the design and optimization of spiral-wound heat exchangers.

2. NUMERICAL METHOD

2.1 Physical model

The geometric profile of spiral-wound heat exchanger is shown in Fig.1. For this heat exchanger, its geometric parameters are determined by diameter d, pitch S, average winding diameter D and number of layers K of the wound tube. The shell length H = 400 mm, the shell diameter D_s = 150 mm and the core barrel diameter D_c = 60 mm of the spiral-wound heat exchanger are used in the actual nuclear power system. Referring to the relevant design manual[11], in order to facilitate manufacturing and winding, the diameter of the wound tube d is usually taking 5-20 mm.

Table 1 shows the main dimensions of the coiled tube heat exchanger and the range of variation of each design variable.

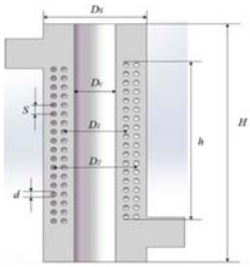

Fig.1 Spiral-wound heat exchanger sectional view

Table1. Main structure parameters of spiral-wound heat exchanger

Structural parameters	*Value*
shell length H/mm	*400*
Shell diameter D_s/mm	*150*
Core barrel diameter D_c/mm	*60*
Wound tube diameter d/mm	*6~15*
Pitch S/mm	*15~30*
Average winding diameter D/mm	*100~110*
Number of layers K	*1~2*
Number of turns n	*8~20*

2.2 Numerical calculation method

According to the Ref.[12], the Realizable k-ε turbulent model can accurately describe the fluid flow in the shell side of spiral-wound heat exchanger. The fluid in the shell is a single-phase continuous fluid and satisfies the following general governing equations[13]:

Continuity equation:

$$\frac{\partial}{\partial x_i}(\rho u_i)=0 \qquad (2\text{-}1)$$

Momentum equation:

$$\frac{\partial}{\partial x_i}(\rho u_i u_k)=\frac{\partial}{\partial x_i}(\mu\frac{\partial u_k}{\partial x_i})-\frac{\partial P}{\partial x_k} \qquad (2\text{-}2)$$

Energy equation:

$$\frac{\partial}{\partial x_i}(\rho u_i t)=\frac{\partial}{\partial x_i}(\frac{\lambda}{C_p}\frac{\partial t}{\partial x_i}) \qquad (2\text{-}3)$$

Turbulent energy equation:

$$\frac{\partial}{\partial t}(\rho k)+\frac{\partial}{\partial x_j}(\rho k u_j)=\frac{\partial}{\partial x_j}\left[\left(\mu+\frac{\mu_t}{\sigma_k}\right)\frac{\partial k}{\partial x_j}\right]+\mu_t\frac{\partial u_i}{\partial x_j}\left(\frac{\partial u_i}{\partial x_j}+\frac{\partial u_j}{\partial x_i}\right)-\rho\varepsilon \qquad (2\text{-}4)$$

Turbulent energy dissipation equation:

$$\frac{\partial}{\partial t}(\rho\varepsilon)+\frac{\partial}{\partial x_k}(\rho\varepsilon u_k)=\frac{\partial}{\partial x_k}\left[\left(\mu+\frac{\mu_t}{\sigma_\varepsilon}\right)\frac{\partial\varepsilon}{\partial x_k}\right]+ \frac{c_1\varepsilon}{k}\mu_t\frac{\partial u_i}{\partial x_j}\left(\frac{\partial u_i}{\partial x_j}+\frac{\partial u_j}{\partial x_i}\right)-c_2\rho\frac{\varepsilon^2}{k} \quad (2\text{-}5)$$

The fluid medium of the shell side is water. The boundary conditions are set as follows:

The inlet is the speed inlet, the fluid temperature is 298K; the outlet uses the pressure outlet boundary condition; The wall surface of the heat exchange tube is set to a constant wall temperature without sliding wall surface, and the wall temperature is 363K; the shell and the core barrel wall are both set as static and non-slip insulating walls, and the wall function is the default standard wall function.

The coupling of pressure and velocity adopts SIMPLE algorithm. The dispersion of pressure term adopts standard format. Momentum, turbulent kinetic energy and turbulent dissipation rate are all adopted in the second-order upwind style. The convergent residual index is set to 1.0×10^-6.

The shell side model of the spiral-wound heat exchanger was meshed using ICEM CFD. Considering the complexity and irregularity of the model geometry, the unstructured tetrahedral mesh was selected in this study. A detailed meshing diagram is shown in Figure 2. In order to ensure the feasibility and accuracy of numerical calculation, mesh independence verification was performed. Considering the calculation accuracy and efficiency, the number of grid cells is selected between 5~6 million under models with different structural.

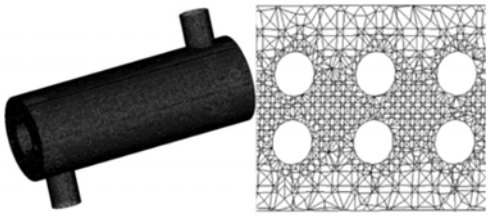

Fig. 2 Mesh model

2.3 Feature parameter definition

Reynolds number Re, Nusselt number Nu, and Friction factor f are used to characterize fluid flow, heat transfer and friction performance of fluid respectively. The definitions of Re, Nu and f are as follows:

$$R_e=\frac{\rho D_e v}{\mu} \quad (2\text{-}6)$$

$$\mathrm{Nu}=\frac{q}{(T_{wall}-T_{ref})}\frac{D_e}{\lambda} \quad (2\text{-}7)$$

$$f=\frac{2\Delta P D_e}{\rho v^2 H} \quad (2\text{-}8)$$

Where ρ is the fluid density, kg/m³; D_e the shell equivalent diameter, m; v the average velocity in the shell side section, m/s; μ the dynamic viscosity, Pa·s; q the fluid heat flux density, W/m²; λ the thermal conductivity, W/(m·K); T_{wall} the wall temperature of the wound tube, K; T_{ref} the average temperature of the shell side fluid K; ΔP the pressure drop of the inlet and outlet, Pa; H the calculated length of the model, m.

3. MULTI-PARAMETER ANALYSIS OF HEAT TRANSFER AND FRICTION PERFORMANCE OF SHELL SIDE

In order to analyze the influence of different structures on the heat transfer and friction performance, the numerical simulation of a large number of shell side models with different structural parameters was carried out.

Fixed the average winding diameter, heat transfer height and winding layers respectively, the variation of Nu and f of shell side with the diameter of wound tube under different pitches is obtained. The range of other structural parameters is shown in Table 1.

3.1 Numerical simulation of shell side

3.1.1 Numerical simulation of shell side under different winding diameters

Fixed K=2, h=270mm, two average winding diameters D=100mm, 110mm were selected, and the variation of Nu and f with the d was obtained under different S as shown in Fig. 3-4.

(a) D=100mm (b) D=110mm

Fig.3 The variation of shell side Nu with D

(a) D=100mm (b) D=110mm

Fig.4 The variation of shell side f with D

Fig.3 and 4 show that Nu increases linearly with the increase of d, decreases with the increase of S, and f decreases with the increase of d, the trend tends to be gentle, and increases with the increase of S. Compared with Fig.3-4 (a), (b), Nu increases with the increase of D under the same S, while f is the opposite. When d is small, the effect of S on fluid resistance is greater, and decreases with increases of D.

3.1.2 Numerical simulation of shell side under different heat transfer height

Fixed K=2 and D=105mm, two heat transfer height h=240mm, 300mm were selected, and the variation of Nu and f with the d was obtained under different S as shown in Fig. 5-6.

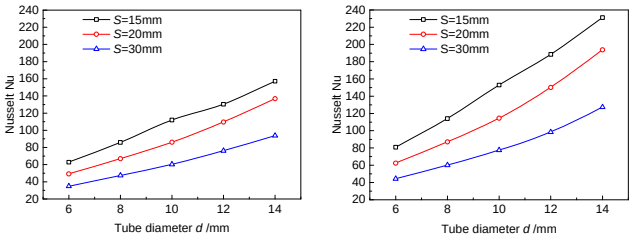

(a) h=240mm *(b) h=300mm*

Fig.5 The variation of shell side Nu with h

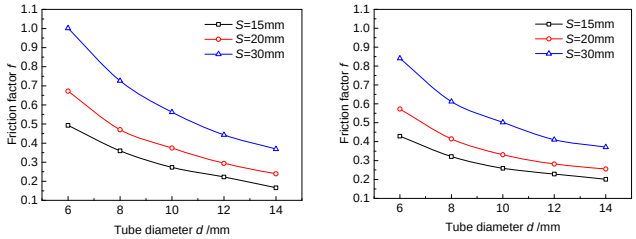

(a) h=240mm *(b) h=300mm*

Fig.6 The variation of shell side f with h

Fig.5 and 6 show that Nu increases linearly with the increase of d, and the increase will gradually increase, especially when h=300mm. Nu decreases with the increase of S, while f is the opposite. The f decreases with the increase of the d, and the downward trend tends to be gentle, and increases with the increase of S. The larger diameter of the wound tube, the more obvious the increasing trend is.

3.1.3 Numerical simulation of shell side under different number of layers

Fixed D=105mm and h=270mm, K=1 and 2 were selected, and the variation of Nu and f with the d was obtained under different S as shown in Fig. 7-8.

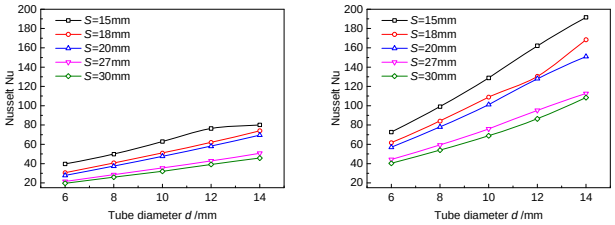

(a) K=1 *(b) K=2*

Fig.7 The variation of shell side Nu with K

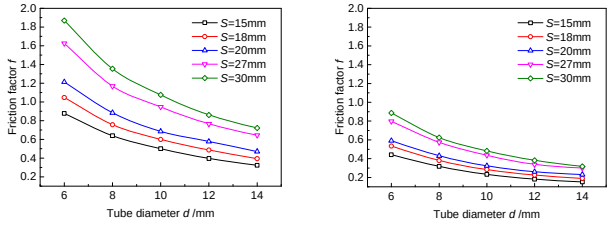

(a) K=1 *(b) K=2*

Fig.8 The variation of shell side f with K

Fig.7 and 8 show that Nu decreases with the increase of S. Compared with Nu, f decreases with the increase of d, and the downward trend tends to be gentle, and increases with the increase of S. When d is small, the trend of f increasing with S is more obvious. Compared with fig.7-8 (a), (b), K has a greater influence on shell side Nu and f than D and h. Under the same S, Nu increases with the increase of K, while f is the opposite. It is shown that increasing K is beneficial to improve the heat transfer and friction performance of the shell side.

3.2 Establishment of new heat transfer correlations

3.2.1 Forms of heat transfer correlations

Nu and f represent heat transfer and friction performance of shell side respectively. The expressions of heat transfer and resistance performance can be written as follows:

$$\mathrm{Nu} = A\mathrm{Re}^{\alpha_1} K^{\alpha_2} n^{\alpha_3} (S/d)^{\alpha_4} (D/d)^{\alpha_5} \qquad (3\text{-}1)$$

$$f = B\mathrm{Re}^{\beta_1} K^{\beta_2} n^{\beta_3} (S/d)^{\beta_4} (D/d)^{\beta_5} \qquad (3\text{-}2)$$

The relationship between the number of turns n and the heat transfer height h in the above numerical simulation is as follows:

$$h = n \cdot S \qquad (3\text{-}3)$$

In order to obtain the values of the coefficients, the numerical simulation is carried out by changing the structural parameters, and the simulation results are shown in the previous section.

3.2.2 Fitting of heat transfer correlations

Based on the numerical results, the SPSS software is used for fitting. The fitting results are as follows:

$$\mathrm{Nu} = 5.534 Re^{0.249} K^{1.248} n^{1.016} (S/d)^{-0.092} (D/d)^{-1.285} \qquad (3\text{-}4)$$

$$f = 0.13Re^{0.127}K^{-0.872}n^{-0.586}(S/d)^{0.337}(D/d)^{0.669} \quad (3\text{-}5)$$

4. VERIFICATION OF NEW HEAT TRANSFER CORRELATIONS

The experimental data in two literatures were compared with the above formulas and other correlations adopted in the literature to verify the accuracy of the new heat transfer correlations.

Firstly, Nu experimental data in Ref. [14] are selected for comparison and verification. The experimental model structural parameters are shown in Table 2.

Table2. structural parameters of experimental model

Model	K	n	d/mm	D/mm	S/mm
1	1	13.5	12	106	17
2	1	10.5	16	102	21.4

The structural parameters of the experimental model are calculated in the Nu correlations (3-4). The Nu experimental values of the two models are compared with the predicted values calculated by using the Nu correlation proposed in this paper and by Srbislav (1-2), Rahul (1-3) as shown in Fig.9-10. The Srbislav correlation only applies to 2000≤Re≤9000. The shadow in the figure is the error band of positive and negative 10% deviation based on the experimental value.

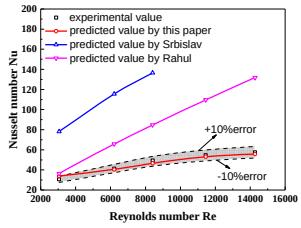

Fig. 9 Model 1 Nu experimental and calculated value comparison

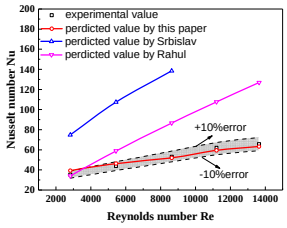

Fig. 10 Model 2 Nu experimental and calculated value comparison

Fig.9-10 shows that the errors between the Nu experimental and predicted values by this paper are basically within the error band. The maximum and minimum errors are 11.35%, 1.88%, which are within the allowable range of engineering. The errors calculated by the other two formulas are larger, which shows that the Nu correlation established in this paper has certain accuracy.

Then, Nu and f experimental data in Ref. [12] are selected for comparison and verification. The experimental model structural parameters is shown in Table 3.

Table3. structural parameters of experimental model

Model	K	n1	n2	d/mm	S1/mm	S2/mm	D/mm
1	2	6	4	12	67	92	109

The Nu and f experimental values are compared with the predicted values calculated by using the correlation proposed in this paper (3-4, 3-5) and by Rahul (1-3), Gilli (1-6) as shown in Fig.11-12.

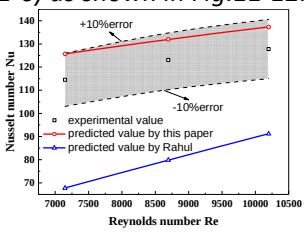

Fig. 11 Nu experimental and calculated value comparison

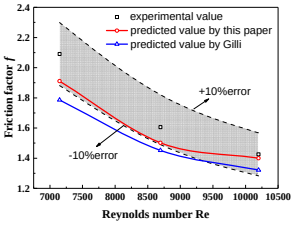

Fig. 12 f experimental and calculated value comparison

Fig.11-12 show that the errors between the Nu and f experimental and predicted values by this paper are basically within the error band. The maximum errors are 9.76%, 8.59%. The errors calculated by the other two formulas are larger.

The verification of new heat transfer correlations show that the errors between the calculated results and the experimental values are small and within the allowable range of engineering. The new heat transfer correlations have certain accuracy and reliability.

5. CONCLUSIONS

In this paper, FLUENT is used to establish the hydrodynamic model of the spiral-wound heat exchangers. The numerical simulation of the shell side is carried out, and the relationship between heat transfer and friction performance is analyzed. Based on the numerical simulation results, the new heat transfer correlations are established, which is verified by the experimental results in literatures. The following conclusions are drawn:

(1) Nu of shell side increases linearly with the wound tube diameter d and decreases with pitch S, while f is the opposite.

(2) Increasing winding diameter D, heat transfer height h, winding layer K, wound tube diameter d or decreasing pitch S are beneficial to improving heat transfer and friction performance of shell side.

(3) Based on the numerical calculation of spiral-wound heat exchangers with different structural parameters, the new heat transfer correlations are established by using the simulation results. The new heat transfer correlations have certain accuracy and reliability. The

new correlations provide the guidance for the design and optimization of the spiral-wound heat exchangers.

[1] Yong-Dong Chen, Xue-Dong Chen. Technology Development of Large-scale Heat Exchanger in China[J]. Journal of Mechanical Engineering, 2013, (10): 134-143.

[2] Zhou-Wei Zhang, Ya-Hong Wang. Spiral Wound Heat Exchanger[M]. Lanzhou: Lanzhou University Press, 2014.

[3] Qing-ye Yu. Research on Calculation Method for Helical Wound Coil Tube Heat Exchangers[D]. Dalian: Dalian University of Technology, 2011: 8-24.

[4] Jia-Xing Xue. Research on Heat Transfer Process of Coil-wound Heat Exchanger[D]. Lanzhou: Lanzhou Jiaotong University.

[5] Zhen Yang, Zhen-Xing zhao, Yin-He Liu, et al. Convective heat transfer characteristics of high-pressure gas in heat exchanger with membrane helical coils and membrane serpentine tubes[J]. Experimental Thermal and Fluid Science, 2011, 35(7):1427-1434.

[6] A. N. Dravid, K. A. Smith, E. W. Merrill, et al. Effect of secondary fluid on laminar flow heat transfer in helically coiled tubes[J]. Aiche Journal, 1971, 17(5): 1114-1122.

[7] Srbislav B, Jaćimović B M, Jarić M S, et al. Research on the shell-side thermal performances of heat exchangers with helical tube coils[J]. International Journal of Heat & Mass Transfer, 2012, 55(15-16): 4295-4300.

REFERENCE

[8] Rahul Kharat, Nitin Bhardwaj, R.S. Jha. Development of heat transfer coefficient correlation for concentric helical coil heat exchanger[J]. International Journal of Thermal Sciences, 2009, 48(12): 2300-2308.

[9] Oi Hua Ying-lang. Handbook of Heat Exchanger Design[M]. Beijing: Petroleum Industry Press, 1984.

[10] Gilli P V. Heat Transfer and Pressure Drop for Cross Flow through Banks of Multistart Helical Tubes with Uniform Inclinations and Uniform Longitudinal Pitches[J]. Nuclear Science & Engineering, 1965, 22(3): 298.

[11] Lanzhou Institute of Petroleum Machinery. Heat Exchanger[M]. Hydrocarbon Processing Press, 1990.

[12] Jing Deng. The Heat Transfer and Flow Characteristics Analysis of Helically Coiled Tube Heat Exchanger[D]. Zhengzhou: Zhengzhou University, 2016.

[13] Fu-Jun Wang. Computational fluid dynamics analysis-principles and applications of CFD software[M]. Beijing: Tsinghua University Press, 2004: 42.

[14] M.R. Salimpour. Heat transfer coefficients of shell and coiled tube heat exchangers[J]. Experimental Thermal and Fluid Science, 2009, 33(2): 203-207.